Anesthesiology 2009; 110:996–1010

Volatile Anesthetic Action in a Computational Model of the Thalamic Reticular Nucleus

Allan Gottschalk, M.D., Ph.D., Sam A. Miotke, M.S.†*

Background: **Although volatile anesthetics (VAs) modulate the activity of multiple ion channels, the process whereby one or more of these effects are integrated to produce components of the general anesthetic state remains enigmatic. Computer models offer the opportunity to examine systems level effects of VA action at one or more sites. Motivated by the role of the thalamus in consciousness and sensory processing, a computational model of the thalamic reticular nucleus was used to determine the collective impact on model behavior of VA action at multiple sites.**

Methods: **A computational model of the thalamic reticular nucleus was modified to permit VA modulation of its ion channels. Isobolographic analysis was used to determine how multiple sites interact.**

Results: **VA modulation of either T-type Ca^{2+} channels or γ-aminobutyric acid type A receptors led to increased network synchrony. VA modulation of both further increased network synchronization. VA-induced decrements in Ca^{2+} current permitted greater impact of inhibitory currents on membrane potential, but at higher VA concentrations the decrease in Ca^{2+} current led to a decreased number of spikes in the burst generating the inhibitory signal. MAC-awake (the minimum alveolar concentration at which 50% of subjects will recover consciousness) concentrations of both isoflurane and halothane led to similar levels of network synchrony in the model.**

Conclusions: **Relatively modest VA effects at both T-type Ca^{2+} channels and γ-aminobutyric acid type A receptors can substantially alter network behavior in a computational model of a thalamic nucleus. The similarity of network behavior at MAC-awake concentrations of different VAs is consistent with a contribution of the thalamus to VA-induced unconsciousness through action at these channels.**

ALTHOUGH it is known that the volatile anesthetics (VAs) modulate activity at a large number of molecular sites,[1,2] it has yet to be determined which of these sites are responsible for general anesthesia (GA) and how action at one or more of these sites leads to the general anesthetic state. Making this determination is further complicated because GA is not a single well-defined phenomenon, but an amalgam of clinically useful effects. These include, in the order they are generally observed as VA concentration is increased, amnesia, unconsciousness, immobility, and blunting of autonomic reflexes. Therefore, the relevancy of a particular molecular site or regions of the central nervous system may depend on which property of GA is being considered.

The property of GA that is most frequently considered is immobility, and this property is generally used to rank VA potency using the minimum alveolar concentration (MAC) of VAs at which 50% of subjects remain immobile in response to a surgical stimulus.[3] As a means of identifying the molecular site of action of the VAs, it was postulated that the concentration–effect curves of the molecular site(s) responsible for GA should match the concentration–effect curve at the systems level.[4] Because the VA concentrations that produce immobility exert relatively modest effects on voltage-gated ion channels,[5–7] this argument seemed to eliminate any of the voltage-gated ion channels as contributors to GA and helped to focus attention on ligand-gated channels such as γ-aminobutyric acid type A ($GABA_A$) receptors, which are modulated by both VAs[8–10] and intravenous anesthetics (IAs).[11–14] Such an argument would seem to have even greater validity for unconsciousness that occurs at VA concentrations (MAC-awake) well below MAC (*e.g.*, 0.25 MAC for isoflurane[15] and 0.59 MAC for halothane,[15] though there is some variability in these determinations[16–20]), where VA effects on ligand-gated channels would also be considerably less. This raises the issue of how small VA effects on ion channels at clinically relevant VA concentrations below MAC can produce meaningful systems level effects. Although computational modeling of neural activity has previously demonstrated how relatively small VA effects can profoundly alter model behavior,[21] this observation has yet to be examined in models relevant to specific features of GA, or those that simultaneously consider VA action at multiple sites.

It is not fully established which networks and which types of network behavior are relevant to the mechanism(s) of GA. However, electroencephalograhic,[22] functional imaging,[23] and pharmacologic studies[24,25] during GA make it clear that the brain is far from quiescent during GA and that GA may be the consequence of anesthetic action at specific anatomic sites within the central nervous system. Within the brain, thalamic activity is altered by the IAs[26,27] and VAs,[23,28] which is consistent with the hypothesized role of the thalamus in sleep and consciousness.[29,30] Overall, these studies demonstrate that during administration of clinically relevant concentrations of IAs and VAs, brain electrical activity

This article is accompanied by an Editorial View. Please see: Pearce RA: All together now. ANESTHESIOLOGY 2009; 110:964–6.

* Associate Professor, † Research Associate.

Received from the Department of Anesthesiology and Critical Care Medicine, Johns Hopkins Hospital, Baltimore, Maryland. Submitted for publication July 23, 2008. Accepted for publication December 30, 2008. Support was provided solely from institutional and/or departmental sources. Presented in part at the Annual Meeting of the American Society of Anesthesiologists, San Francisco, California, October 15, 2007.

Address correspondence to Dr. Gottschalk: Department of Anesthesiology and Critical Care Medicine, Meyer 8-134, Johns Hopkins Hospital, 600 North Wolfe Street, Baltimore, Maryland 21287. agottschalk@jhmi.edu.

continues but often becomes more synchronous, and this can manifest itself in slowing of electroencephalographic activity.

If, in fact, the thalamus does play a role in VA induction of unconsciousness, it is reasonable to hypothesize that this is due to known VA actions at T-type Ca^{2+} channels[6] and/or $GABA_A$ receptors,[8–10] which are anesthetic-sensitive voltage- and ligand-gated ion channels that dominate, respectively, many intrinsic and network properties of thalamic neurons.[29,31–33] However, as already emphasized, at MAC-awake concentrations of the VAs, these effects are limited. This raises the possibility of interaction between multiple VA sites of action if anesthetic action at these channels in the thalamus contributes to loss of consciousness. VA action at both voltage- and ligand-gated thalamic channels is consistent with the putative contribution of the thalamus to consciousness in that isoflurane is more potent than halothane at both T-type Ca^{2+} channels and $GABA_A$ receptors,[6,8,34,35] and isoflurane, though less potent than halothane with respect to immobility, is, in fact, more potent than halothane with respect to MAC-awake.[15–20]

To better assess how established VA effects on ion channels can impact thalamic function at VA concentrations known to affect consciousness, a computational model of the isolated thalamic reticular nucleus (RTN) was examined. Because the characteristic behavior of the RTN plays an important role in regulating thalamic oscillations[36] and is dominated by the behavior of T-type Ca^{2+} channels and $GABA_A$ receptors,[29,32,33,37] the impact of VA action on network behavior of the RTN was examined for these sites individually and in concert.

Materials and Methods

Neural Model

A model of the RTN (fig. 1) was generated from a single compartment model of individual neurons based on previous models.[32,33,37] In addition to a leak current, membrane currents included the slow T-type Ca^{2+} channel present in neurons of the RTN, a fast Na^+ channel, and a delayed rectifier K^+ channel. Networks of individual neurons were connected with $GABA_A$ synapses using a random pattern of connectivity.

The voltage in each neuron was modeled using the relation

$$C_i \frac{dV_i}{dt} = I_{inject\text{-}i} - I_{ion\text{-}i} - \sum_{k=1}^{N} I_{GABA_{A}-ik} \qquad (1)$$

where C_i is the membrane capacitance of the i-th neuron, V_i is the membrane potential of the i-th neuron, $I_{inject\text{-}i}$ is the injection current to the i-th neuron, $I_{ion\text{-}i}$ is the sum of ionic currents due to the leak and voltage-gated channels in the i-th neuron, and the $I_{GABA_{A}-ik}$ are

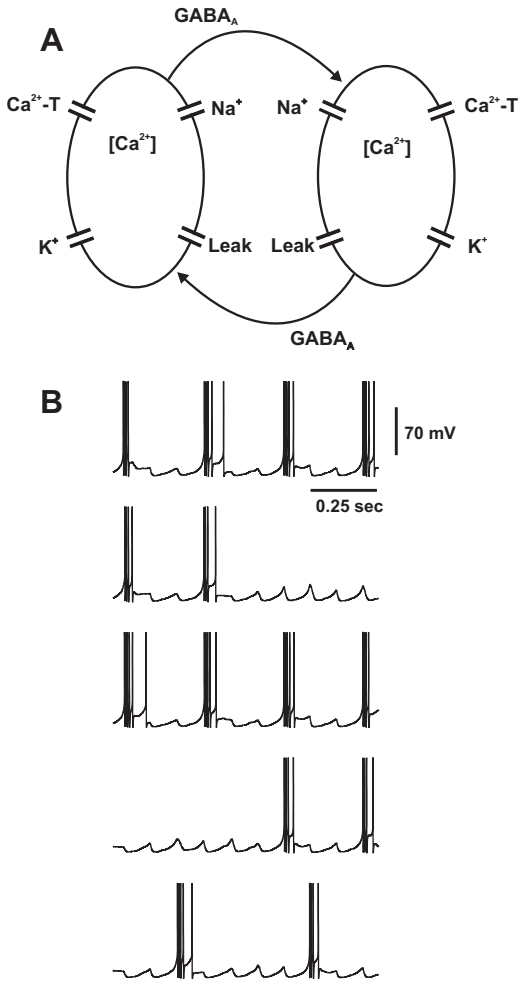

Fig. 1. Schematic of computational model (*A*) and representative examples of membrane potentials from individuals network neurons (*B*). Single compartment models of neurons of the reticular nucleus of the thalamus are coupled by inhibitory γ-aminobutyric acid type A ($GABA_A$) synapses. Each neuron contains a T-type Ca^{2+} channel, a fast Na^+ channel, a delayed rectifier K^+ channel, a leak current, and a membrane capacitance. The Ca^{2+} current modulates internal Ca^{2+} concentration, which, in turn, modulates Ca^{2+} reversal potential. Each of the 100 neurons in the model is randomly coupled, on average, to 85% of the other neurons in the network (excluding self) with a fixed value of $GABA_A$ conductance. Neural activity generally consists of bursts of action potentials riding on the depolarization produced by the T-type Ca^{2+} channel. Bursting occurs in response to postinhibitory rebound of the membrane potential.[32,33,42] Each action potential in a burst generates a synaptic pulse of GABA. Note how some neurons are in phase whereas others are not. Also note the presence of subthreshold oscillations in membrane potential due to inhibitory input from other neurons in the network.

the $GABA_A$ currents from any other neurons that make synaptic contacts with the i-th neuron. The ionic currents are modeled using the general formula

$$I_{ion\text{-}ij} = \bar{g}_{ij}\, m_{ij}^{pj}\, h_{ij}^{qj} \left(V_i - V_{rev\text{-}ij}\right) \qquad (2)$$

where $I_{ion\text{-}ij}$ is the j-th ionic current in the i-th neuron, g_{ij} is the maximum conductance of that current, m_{ij} is the corresponding activation variable, h_{ij} is corresponding inactivation variable, p_j is the power associated with activa-

tion of the j-th ionic current, q_j is the power associated with inactivation of the j-th ionic current, and $V_{rev\text{-}ij}$ is the corresponding reversal potential. The general form for both the activation and inactivation variables is

$$\frac{dm_{ij}}{dt} = \alpha(V_i)(1 - m_{ij}) - \beta(V_i)m_{ij} \quad (3)$$

where $\alpha(V_i)$ is the opening rate of the corresponding variable and $\beta(V_i)$ is the corresponding closing rate, which are generally voltage dependent. In general, the reversal potential is fixed for each of the ions except for Ca^{2+}, whose reversal potential is a function of the internal Ca^{2+} concentration. Here, the reversal potential for Ca^{2+} is given by the Nernst equation,

$$V_{rev\text{-}iCa} = \frac{RT}{z_{Ca}F} \ln \frac{[Ca]_{out}}{[Ca]_{in\text{-}i}} \quad (4)$$

where $z_{Ca} = 2$ is the charge on the Ca^{2+} ion, $F = 9.648 \times 10^4$ C mol^{-1} is the Faraday constant, $R = 8.315$ J K^{-1} mol^{-1} is the gas constant, T is the temperature in K, $[Ca^{2+}]_{in\text{-}i}$ is the internal Ca^{2+} concentration in the i-th neuron in millimoles, $[Ca^{2+}]_{out}$ is the external Ca^{2+} concentration in millimoles, and ln[·] is the natural logarithm. Modulation of the internal Ca^{2+} concentration by the Ca^{2+} current is given by

$$\frac{d[Ca^{2+}]_{in\text{-}i}}{dt} = -\frac{k}{hFz_{Ca}} I_{ion\text{-}iCa} - \frac{[Ca^{2+}]_{in\text{-}i} - c}{\tau_{Ca}} \quad (5)$$

where h is the thickness in μm of the internal shell whose concentration is of interest, c is the equilibrium value of $[Ca^{2+}]_{in\text{-}i}$, k is a constant to permit the units to be correct, and τ_{Ca} is the time constant governing the achievement of the equilibrium concentration.

For networks coupled by $GABA_A$ synaptic interactions, each spike generated by a presynaptic neuron produced a fixed pulse of GABA of 0.5 mM and 0.3 ms duration at the postsynaptic neuron, increasing the concentration of GABA in the synapse.[33] The kinetics governing activation of the $GABA_A$ receptor becomes

$$\frac{dm_{GABA_A-i}}{dt} = \alpha[GABA](1 - m_{GABA_A-i}) - \beta m_{GABA_A-i} \quad (6)$$

where [GABA] is the concentration of GABA in the synapse, and α and β are the rate constants governing opening and closing of the $GABA_A$ receptor. Typically, in the absence of anesthetic effects, $\alpha = 20$ ms^{-1} mM^{-1} and $\beta = 0.16$ ms^{-1}.[33]

The specific form of the rate parameters and exponents of the activation variables of equation 2 for the slow T-type Ca^{2+}, Na^+, and K^+ ion channels have been specified previously along with the model parameters described subsequently.[33] The membrane capacitance was 1 $\mu F/cm^2$. The baseline Ca^{2+} conductance used was

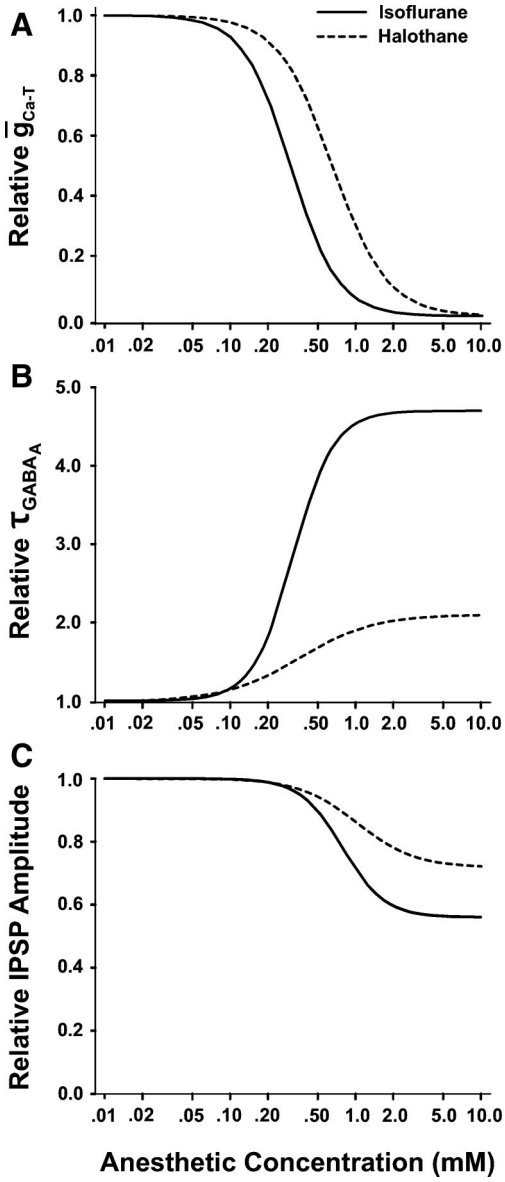

Fig. 2. Volatile anesthetic effects on T-type Ca^{2+} channels and γ-aminobutyric acid type A ($GABA_A$) receptors for both isoflurane (*solid line*) and halothane (*dashed line*). The normalized decrease in T-type Ca^{2+} channel conductance is shown as a function of volatile anesthetic concentration in *A*. The values of the Hill exponent and semisaturation constant used in equation 7 are, respectively, n = 2.3 (±0.15) and $[A]_{1/2} = 0.30$ (±0.01) for isoflurane, and n = 2.0 (±0.10) and $[A]_{1/2} = 0.66$ (±0.03) for halothane.[6] The relative increase in the time constant governing deactivation of the $GABA_A$ receptor as anesthetic concentration is increased is shown in *B*. Here, the maximum prolongation of the time constant, the Hill exponent, and the semisaturation constant used in equation 8 are, respectively, $f_{max} = 4.7$ (±0.50), n = 2.7 (±1.2), and $[A]_{1/2} = 0.32$ (±0.05) for isoflurane,[8] and $f_{max} = 2.1$ (±0.51), n = 1.5 (±1.0), and $[A]_{1/2} = 0.36$ (±0.26) for halothane.[8,34,35] The decrease in the amplitude of the inhibitory postsynaptic potential (IPSP) at the $GABA_A$ receptor as anesthetic concentration is increased is shown in *C*. The values of the Hill exponent, semisaturation constant, and maximum IPSP attenuation used in equation 9 are, respectively, n = 2.6 (±0.80), $[A]_{1/2} = 0.79$ (±0.24), and $y_{max} = 0.56$ (±0.13) for isoflurane,[8] and n = 1.9 (±1.0), $[A]_{1/2} = 1.0$ (±0.36), and $y_{max} = 0.72$ for halothane, where the value for y_{max} for halothane was obtained from a single point.[8,35]

3 mS/cm^2, the Na^+ conductance used was 200 mS/cm^2, the K^+ conductance used was 20 mS/cm^2, and the leak conductance used was 0.05 mS/cm^2. The reversal potentials were $V_{Na} = 50$ mV, $V_K = -100$ mV, $V_L = -90$ mV, and $V_{Cl} = -80$ mV (reversal potential of $GABA_A$ current). The external Ca^{2+} concentration was assumed to be 2 mM. The resting internal Ca^{2+} concentration was assumed to be 2.4×10^{-4} mM at equilibrium, and τ_{Ca} was 5 ms. The surface area of the neuron was 1.41887×10^{-4} cm^2, the thickness of the internal shell h was 0.1 μm, and the constant k was 0.1. As described in the Results, the remaining parameters were tuned to provide model behavior suitable for examining alterations in network synchrony by the VAs (*e.g.*, initial state neither perfectly synchronous nor asynchronous). The synaptic conductance of the inhibitory $GABA_A$ synapses was set to $0.2/N_{Conn}$ μS, where N_{Conn} is the expected number of connections in the randomly connected network of N neurons. The number of neurons was 100 with 85% connectivity so that N_{Conn} was 85. A bias current of 0.12 nA was applied to all neurons to simulate exogenous excitatory input. All simulations were performed at 36°C. Examples of the behavior of representative neurons from this model of the RTN before introducing VAs are given in figure 1 along with the model schematic.

Anesthetic Effects

Multiple VA effects on both the voltage- and ligand-gated ion channels are known.[1,2] The nature and magnitude of the interaction can be highly specific to the channel and can vary with the anesthetic. The Ca^{2+} channel seems to be the most sensitive of the voltage-gated ion channels considered in the current model.[4,5] Although the VAs seem to affect the dynamics of activation and inactivation of the L- and N-type Ca^{2+} channels,[5,38] these features are minimally affected for the T-type channels.[6] Consequently, VA action at these channels is modeled by modulating the conductance as a function of VA concentration using the Hill equation to fit existing experimental data. Therefore, the current in the channel is modified by multiplication with the function

$$\phi([A]) = \frac{[A]_{1/2}^n}{[A]^n + [A]_{1/2}^n} \quad (7)$$

which is one when the anesthetic concentration [A] is zero, and goes to zero as [A] continues to increase. Here, n is the Hill exponent and $[A]_{1/2}$ is the semisaturation constant, the value of [A] where $\phi([A]) = 1/2$. Examples of $\phi([A])$ for halothane and isoflurane are shown in figure 2A. VA decrements in the currents produced by the fast Na^+ and the delayed rectifier K^+ are known,[5] but they are small and have had little impact when incorporated into a simplified computational model of the CA3 hippocampal neuron.[21] In addition to its direct effect on the ion channel, VA modulation of Ca^{2+} channel activity affects internal Ca^{2+} concentration, which modulates the Ca^{2+} reversal potential.

Like many of the IAs, some of the VAs can also prolong the time constant ($\tau_{GABA_A} = 1/\beta$ for β in equation 6) governing deactivation of the $GABA_A$ receptor.[8,34,35] The Hill equation has been used to characterize these effects, so that β in equation 6 is adjusted by dividing it by the expression

$$\psi[A] = 1 + (f_{Max} - 1)\frac{[A]^n}{[A]^n + [A]_{1/2}^n} \quad (8)$$

where f_{max} is the maximum possible increase in the time constant governing deactivation of the $GABA_A$ receptor. Examples of the increase τ_{GABA_A} for halothane and isoflurane are shown in figure 2B.

The VAs can also decrease amplitude of the inhibitory postsynaptic potential (IPSP) generated by GABA at the $GABA_A$ receptor. This can be addressed in much the same way that reductions in other ionic currents were addressed, but by modifying equation 7 to reflect that the amplitude of the IPSP does not go to zero as VA concentration increases,[17,23] using the following equation:

$$\zeta([A]) = 1 - (1 - y_{Max})\frac{[A]^n}{[A]^n + [A]_{1/2}^n} \quad (9)$$

where y_{max} is the relative IPSP amplitude at maximum attenuation. Examples of the reductions in the IPSPs generated at the $GABA_A$ receptor due to VAs are given in figure 2C. From this, it can be seen that at lower VA concentrations VA reductions in IPSP amplitude are minimal. Therefore, at the $GABA_A$ receptor, the VA effect of decreasing the rate of receptor deactivation is dominant.

Computer Simulations and Analysis

Simulations of single neurons and small networks were performed using Mathematica (Wolfram Research, Champaign, IL)[39] on a personal computer based on an Intel Pentium IV processor (Dell, Inc., Round Rock, TX) running Windows XP (Microsoft Corporation, Redmond, WA), and larger network simulations were performed using the neural simulation language GENESIS‡ using a computer based on a Xenon Quad-Core processor (Western Scientific, San Diego, CA) with the Linux operating system (Red Hat, Raleigh, NC).

Network activity was initiated by stimulating each neuron with a single randomly generated inhibitory current pulse with an occurrence time uniformly distributed over 1 s and with an amplitude uniformly distributed between 0 and 0.2 nA. After this initial second, network behavior was permitted to evolve for an additional 5 s before generating data for analysis. When estimating properties of network behavior from multiple simulations with the same parameters, simulations were performed using a different random

‡ General Neural Simulation System. Available at: www.genesis-sim.org/GENESIS.[40] Accessed March 27, 2009.

seed to generate both network connectivity and the random pulse sequence used to initiate network activity.

Overall network behavior was quantified in a number of ways. Raster plots were generated, which graphically indicate the membrane potential of all neurons in the network over time by converting the membrane potential of each to a grayscale variable and simultaneously plotting all of these. Network synchrony can be further visualized by examining the relative phase of each neuron in the network. This was accomplished using Fourier analysis.[41] The Fourier transform of the membrane potential from each neuron was computed from 3 s of data, and the dominant frequency of each was determined from the location of the maximum peak in the power spectrum. Then, for this frequency, the phase was computed from the Fourier transform. The results for the entire network were summarized in a histogram. The average membrane potential was computed to simulate the field potential of an appropriately located depth electrode by simply averaging the individual potentials of all neurons within the network. The autocorrelation function of the averaged membrane potential was also determined. A coherence parameter (χ^2) computed from the same 3 s of data was used to quantify network synchrony with a single parameter.[42] This is done using the following coherence function:

$$\chi^2 = \frac{\frac{1}{T}\int_0^T [\overline{V}(t) - \overline{V}]^2 \, dt}{\frac{1}{N}\sum_{i=1}^{N} \frac{1}{T}\int_0^T [V_i(t) - \overline{V}_i]^2 \, dt}$$

where

$$\overline{V}(t) = \frac{1}{N}\sum_{i=1}^{N} V_i(t) \qquad (10)$$

$$\overline{V} = \frac{1}{T}\int_0^T \overline{V}(t)dt$$

$$\overline{V}_i = \frac{1}{T}\int_0^T V_i(t)dt$$

where $V_i(t)$ is the membrane potential of the i-th neuron, and T is the duration of the interval under consideration. χ^2 Can range between zero (no synchrony) and one (perfect synchrony), and is the ratio of variation of the overall average membrane potential around the overall mean to the average of the individual membrane potentials around their individual means.

Results

Joint Sensitivity to the Volatile Anesthetics

Using the data from figure 2, as the concentrations of the VAs isoflurane and halothane are increased, a locus for each is described in the plane defined by relative decrements in conductance of T-type Ca^{2+} conductance and increases in the time constant (τ_{GABA_A}) governing the rate of $GABA_A$ receptor deactivation (fig. 3). Note the proximity of the clinically determined values for MAC-awake (the minimum alveolar concentration at which 50% of subjects will recover consciousness) for these two VAs. This is consistent with the hypothesis that action at these sites may be associated with VA effects on consciousness in brain regions, such as the thalamus, whose behavior is dominated by T-type Ca^{2+} channels and inhibitory $GABA_A$ interactions.

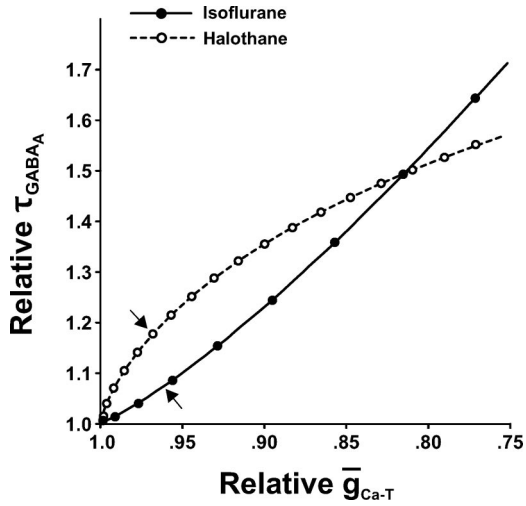

Fig. 3. Loci of volatile anesthetic effects for decrements in conductance of T-type Ca^{2+} channels and increase in the time constant (τ_{GABA_A}) governing γ-aminobutyric acid type A ($GABA_A$) receptor deactivation for both isoflurane and halothane as volatile anesthetic concentration is increased. *Symbols* (● = isoflurane, ○ = halothane) correspond to increments of 0.02 mM volatile anesthetic concentration. *Arrows* denote locations of MAC-awake (0.075 mM = 0.25 MAC for isoflurane and 0.12 mM = 0.59 MAC for halothane),[15] where MAC is the minimum alveolar concentration at which 50% of subjects remain immobile to incision (0.3 mM for isoflurane and 0.2 mM for halothane). The fractional decrease in T-type Ca^{2+} conductance is shown on the *horizontal axis*, and the fractional increase of the time constant (τ_{GABA_A}) governing $GABA_A$ receptor deactivation is shown on the *vertical axis*. The *origin* corresponds to an anesthetic concentration of zero.

Volatile Anesthetic Action on Biophysical Model of the RTN

Volatile anesthetic action at both T-type Ca^{2+} channels and $GABA_A$ receptors as quantified in figure 2 can increase the level of synchrony in the biophysical model of the RTN at clinically relevant VA concentrations. This is shown in figure 4 for both isoflurane and halothane at VA concentrations of twice MAC-awake. In figure 4, the raster plots depict the firing pattern for all 100 neurons in the network over time under control conditions and in the presence of anesthetic effects attributable to 0.15 mM isoflurane and 0.24 mM halothane. This demonstrates how relatively modest VA effects can noticeably alter the behavior of this model but does not indicate whether the

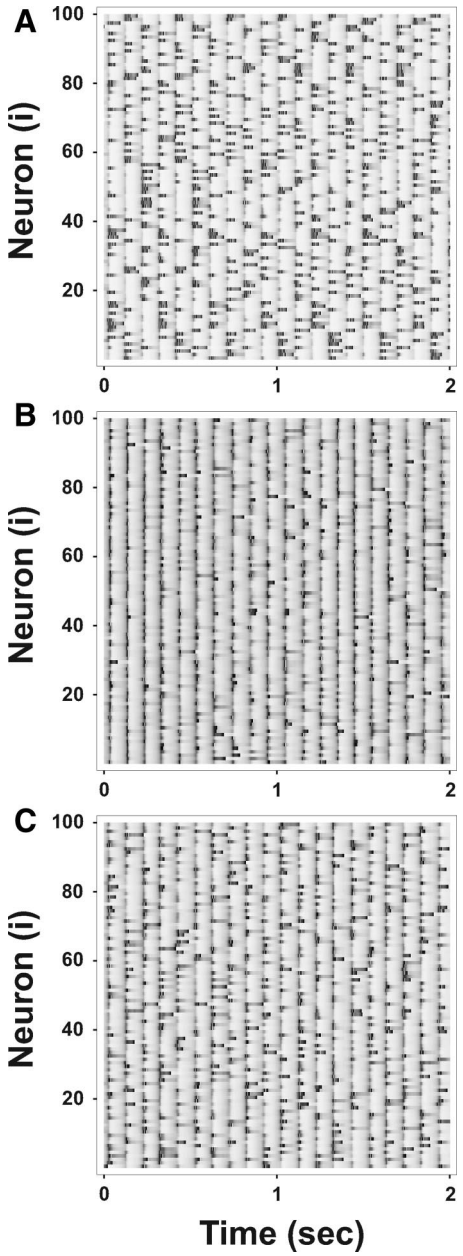

Fig. 4. Synchronization of model network activity by the volatile anesthetic actions of figure 2. Raster plots depicting the activity of all 100 neurons in the network are shown for control conditions (*A*) and at twice minimum alveolar concentration (MAC)-awake for two different volatile anesthetics (0.15 mM isoflurane [*B*] and 0.24 mM halothane [*C*]). Volatile anesthetic effects included decreasing T-type Ca^{2+} channel conductance and an increase in the time constant (τ_{GABA_A}) governing γ-aminobutyric acid type A ($GABA_A$) receptor deactivation. The activity of each of the 100 neurons in the network is depicted over time by continuously mapping membrane potential to grayscale intensity, where darker intensity denotes larger values of membrane potential. Note the ability of clinically relevant volatile anesthetic concentrations to synchronize network activity (*e.g.*, more membrane activity at a given phase) and that pattern of activity seems more organized for isoflurane (*B*) than for halothane (*C*).

alterations in model behavior are due to VA effects at the T-type Ca^{2+} channel, the $GABA_A$ receptor, or both.

The contribution of the individual VA effects can be evaluated by considering their impact on model behavior individually and collectively. This is done and further quantified in figure 5 for the same VA concentrations as in figure 4. Here, network behavior for each condition is depicted by the average membrane potential, which is the model equivalent of the local field potential or electroencephalogram. Average membrane potential was generated by averaging the individual membrane potentials from all neurons in the network. Despite the obvious alterations in synchrony of the model neurons in figure 4, the alterations in the average membrane potential are subtle and are not further revealed by autocorrelation (not shown). However, other measures shown in figure 5 demonstrate the extent to which neural activity becomes more organized. The histogram shown in each panel indicates the number of neurons that are active for a given relative phase of the network's fundamental frequency of activity. Increased synchrony would be indicated by a greater number of neurons firing at the same or similar phases. It is convenient to quantify the degree of network synchrony with a single parameter using the coherence parameter described in the Materials and Methods.[42] An increase in network synchrony is indicated in figure 5 by slowing and increased amplitude of the oscillations in average membrane potential, a greater number of neurons at a similar phase, and an increase in the coherence (χ^2). An increase in the synchrony of model activity was observed for VA effects on T-type Ca^{2+} channels alone, $GABA_A$ receptors alone, and both T-type Ca^{2+} channels and $GABA_A$ receptors. However, at least for the VA concentrations depicted in figure 5, synchronous activity is greatest when VA effects are applied to both sites. Note also in figure 5 that the coherence values for both isoflurane and halothane are greater than for control conditions and that for isoflurane is greater than that for halothane, all of which is consistent with the appearance of the raster plots of figure 4.

The results of figure 5 are expanded in figure 6, where coherence is computed as a function of the relative conductance of the T-type Ca^{2+} channel with respect to its baseline, relative increases in τ_{GABA_A}, and as a function of anesthetic concentration for isoflurane and halothane. The results from figures 6C and D are rescaled in figures 6E and F to depict network synchrony as a function of MAC fraction and to demonstrate the similarity of the coherence parameter for isoflurane and halothane for VA concentrations corresponding to MAC-awake.

Synergy of VA Effects at Multiple Targets

To characterize the nature and extent of VA effects at T-type Ca^{2+} channels and $GABA_A$ receptors across a range of VA concentrations, an isobologram for each VA can be generated for the model[43,44] using the coherence measure in equation 10 as the quantifiable drug effect. In this particular instance, the process of generating an isobologram is somewhat restricted because both drug

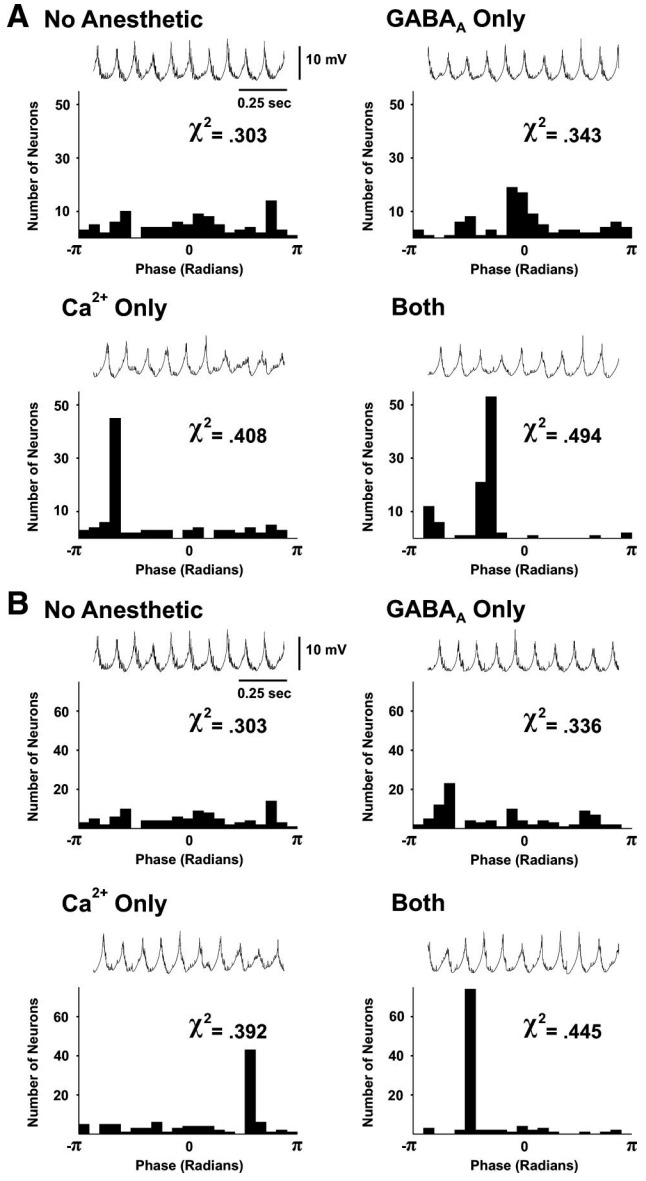

Fig. 5. Characteristics of the network synchronization by volatile anesthetics depicted in figure 4 for both 0.15 mM isoflurane (*A*) and 0.24 mM halothane (*B*). Model behavior is shown for control (no volatile anesthetic, *upper left panel*), VA-induced decrease in T-type Ca^{2+} channel conductance only (*lower left panel*), volatile anesthetic–induced increase in the time constant (τ_{GABA_A}) governing γ-aminobutyric acid type A ($GABA_A$) receptor deactivation only (*upper right panel*), and actions at both of these sites (*lower right panel*). For each condition, the field potential of the network, a numeric measure of network synchrony (coherence, χ^2), and a histogram of relative phase are shown. Note how volatile anesthetic actions at either the voltage-gated site or ligand-gated site leads to increasingly organized network behavior with each of these measures, and that organized behavior seems to be the greatest for action at both sites. Note also that although the histogram for halothane when both channels are considered demonstrates greater similarity of phase in the histogram than isoflurane, the χ^2 value is lower. Here, the level of synchrony as reflected by χ^2 is more consistent with what is seen in figure 4 and emphasizes the importance of using a synchrony measure such as χ^2 that considers both phase and amplitude at all frequencies, as highlighted in the Discussion in the section Characterizing Network Behavior. Scales for both voltage and time are given in the *upper left panel* of each. See text for details.

effects are not manipulated separately by varying independently the concentration of two different drugs. Instead, both effects vary jointly as a function of anesthetic concentration as shown in figure 3, and joint effects are restricted to the loci shown there. However, the computational approach illustrated in figures 5 and 6 demonstrates how VA effects on the model can be examined individually and then jointly for the combinations permitted by each VA as its concentration is increased.

The data in figures 3 and 6 were used to generate the isoboles which collectively form the isobolograms shown in figure 7. For each anesthetic concentration along the loci of figure 3, the coherence of the network was determined from the data given in figures 6C and D. Then, the relative attenuation of the T-type Ca^{2+} conductance and relative prolongation in the time constant for $GABA_A$ receptor deactivation that would produce the same level of network coherence were determined using the equations fit in figure 6A and B. The line connecting these three points is an isobole, and generating these for multiple anesthetic concentrations produced the isobolograms of figure 7.

The isobolograms for isoflurane and halothane, separately and together, are shown in figure 7. An isobole forming a straight line indicates additivity, whereas isoboles concave with respect to the origin indicate some degree of synergism and those convex with respect to the origin indicate some degree of antagonism.[43] For the VAs, there is no single pattern of interaction individually or collectively. What is most apparent is that there is meaningful interaction over the range of simulations studied that is largely additive.

Mechanism of Interaction

The T-type Ca^{2+} channel conductance contributes to the intrinsic properties of individual neurons, and the $GABA_A$ receptor is responsible for network interactions. However, figure 6A and the isobolograms of figure 7 demonstrate that VA modulation of Ca^{2+} channel conductance can also affect synchronization of the model network. Reductions in T-type Ca^{2+} conductance will reduce membrane depolarization by the Ca^{2+} channel and permit the inhibition produced by a given level of $GABA_A$ activation to produce a relatively greater reduction in membrane potential than when it is applied while the Ca^{2+} current is larger. The significance of this with respect to network synchronization is shown in figure 8, where a reduction in the T-type Ca^{2+} conductance allows a GABA pulse to increase the resultant delay in the firing of a single neuron firing without network influence. The conductance from a single synapse from a presynaptic neuron in the network corresponds to approximately 0.002 μS. As shown in figure 8, as the $GABA_A$ receptor conductance increases, so does the delay due to a single GABA pulse. By enhancing the effectiveness of an inhibitory pulse in preventing the firing of

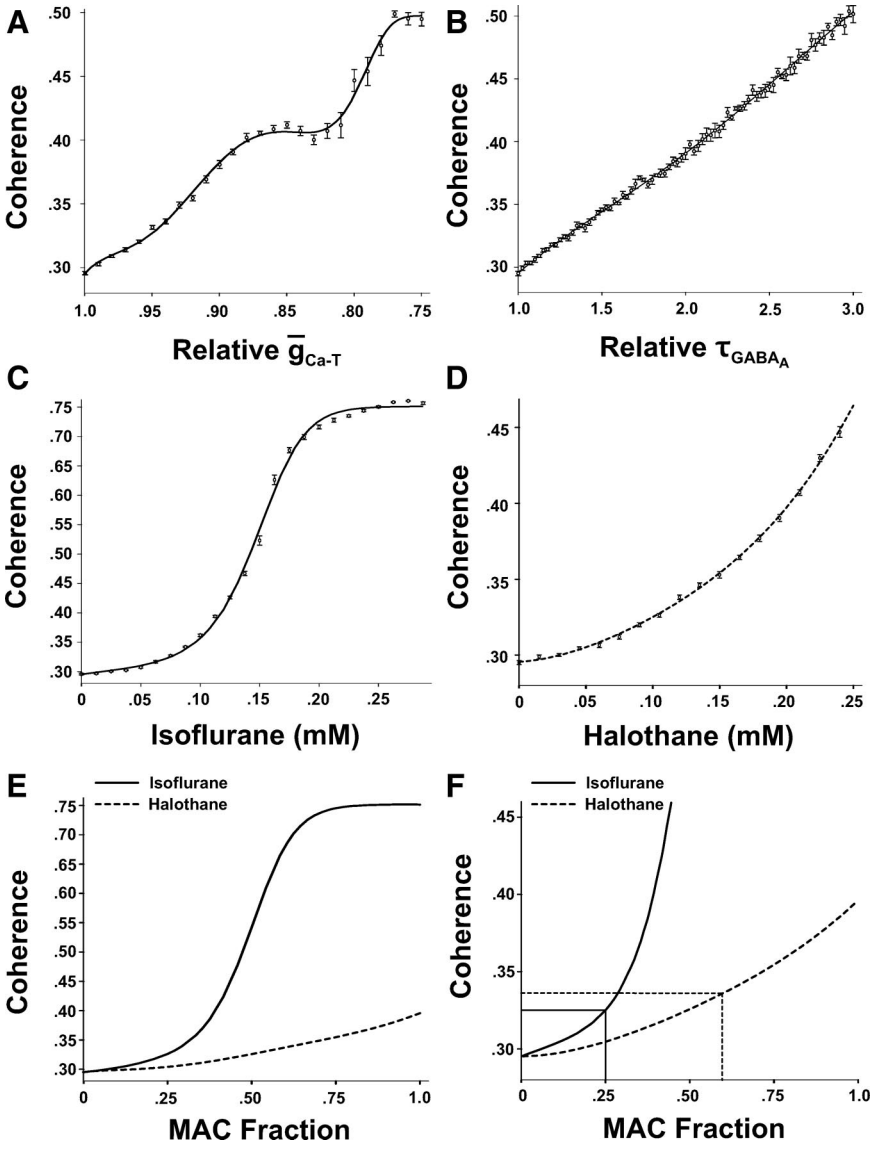

Fig. 6. Network coherence (χ^2) as channels in the model are modulated one type at a time, and when these effects are considered together for the volatile anesthetics isoflurane and halothane. Network coherence is shown for decrements in the conductance of the T-type Ca^{2+} channel (*A*), and as the time constant (τ_{GABA_A}) governing the rate of γ-aminobutyric acid type A ($GABA_A$) receptor deactivation is increased (*B*). Network coherence was also determined as a function of isoflurane concentration (*C*) and halothane concentration (*D*) using the combined effects of each volatile anesthetic on the T-type Ca^{2+} conductance and the time constant (τ_{GABA_A}) governing the rate $GABA_A$ receptor deactivation that is depicted in figures 2 and 3. Each *point* is the mean (±SEM) value of χ^2 obtained from either 6 (*B*) or 12 (*A*, *C*, and *D*) simulations differing only in their randomly assigned pattern of connectivity and timing of initial current pulses to the network (see Materials and Methods). Each curve was obtained from a least-squares fit of the simulation data to the equation $f(x) = V/(1 + e^{-g(x)}) + k$, where $g(x) = a_0 + a_1x + a_2x^2 + \ldots a_dx^d$, where the degree d was either 5 (*A–C*) or 4 (*D*). The data from *C* and *D* are plotted jointly in *E* but expressed in multiples of minimum alveolar concentration (MAC) for both isoflurane (MAC = 0.3 mM) and halothane (MAC = 0.2 mM), which is rescaled (*F*) to demonstrate the similarity of the coherence for each volatile anesthetic's MAC-awake concentration (0.25 MAC for isoflurane and 0.59 MAC for halothane). Here, χ^2 was 0.325 for isoflurane and 0.335 for halothane at the MAC-awake concentrations of these volatile anesthetics. Note that the control value of χ^2 is 0.295. For MAC-awake concentrations of the volatile anesthetics acting on one channel at a time, isoflurane increases χ^2 to 0.304 when affecting the $GABA_A$ receptor alone and 0.320 when affecting the T-type Ca^{2+} channel alone. Similarly, halothane increases χ^2 to 0.316 when acting only at either the $GABA_A$ receptor or T-type Ca^{2+} channel.

a postsynaptic neuron, the window in time where neural activity is more probable becomes smaller, making it more likely that activity will occur at more similar phases and synchronize. This effect exerts a greater impact on network synchrony once several neurons start to fire in concert (simulated in fig. 8 by increases in conductance of the $GABA_A$ receptor). When these results are considered within a larger network, it can be seen that reductions in T-type Ca^{2+} conductance make the inhibitory interactions in the network effectively stronger, leading to greater network synchrony. However, the effect on synchronization of decreasing the T-type Ca^{2+} conductance is constrained. As shown in figure 9, the average number of spikes per burst decreases as the T-type Ca^{2+} conductance is decreased. This decrease in the burst length decreases the inhibition generated in the postsynaptic neuron because each action potential in the burst generates a synaptic pulse of GABA. However, some of the decrease in burst length as the T-type Ca^{2+} conductance decreases is overcome by simultaneous arrival of multiple inhibitory pulses as network synchrony increases. Network coherence as the T-type Ca^{2+} conductance is decreased in figure 6A could be interpreted as a balance of the effects shown in figures 8 and 9.

Sensitivity of Model Assumptions

Because the results already presented could depend heavily on the assumptions and parameters that underlie the model, a number of these were examined. These included the level of bias current exciting each neuron, use of a randomly distributed bias current, the average fraction of neurons to which each neuron is connected, the conductance of the $GABA_A$ receptor, the presence of the small conductance Ca^{2+}-dependent K^+ channel

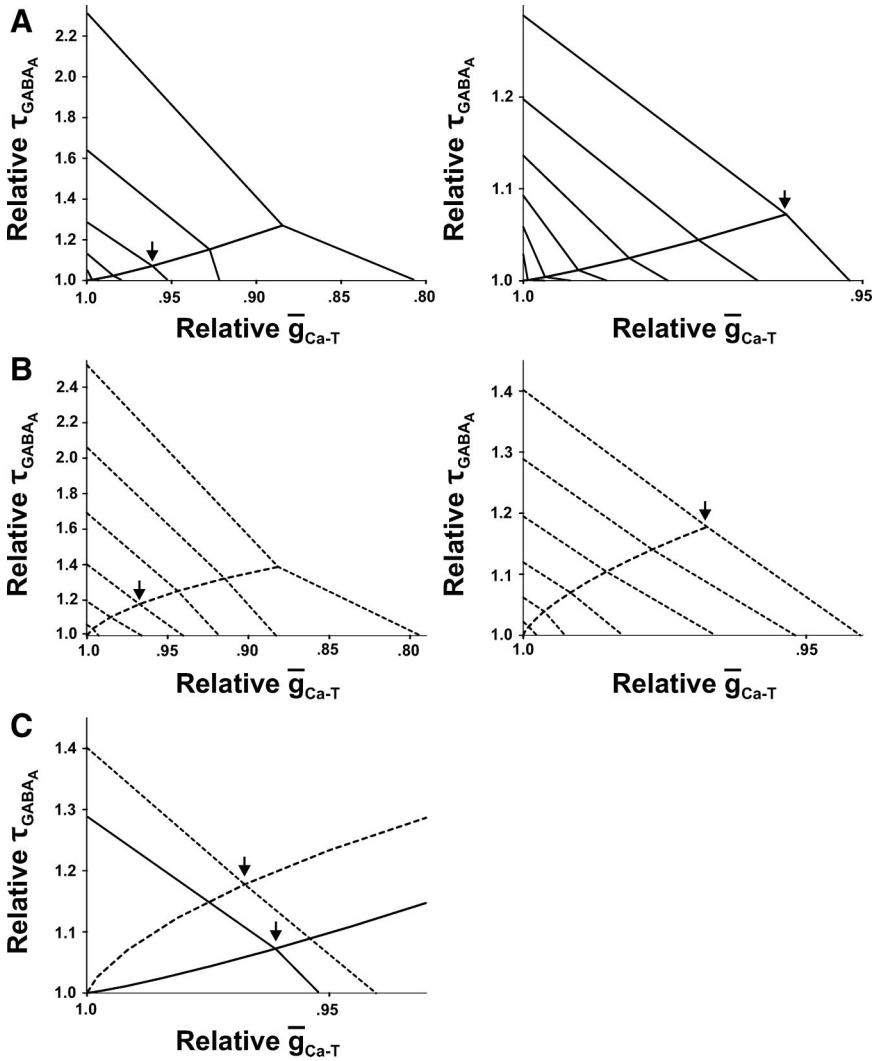

Fig. 7. Isobolograms for isoflurane (*A*) and halothane (*B*) using network synchronization as the drug effect for combinations of decreases in T-type Ca^{2+} channel conductance and increases in the time constant (τ_{GABA_A}) governing γ-aminobutyric acid type A ($GABA_A$) receptor deactivation that correspond to the actions of the volatile anesthetics. The isobolograms were generated using the data of figure 6 and the loci of figure 3 to define pharmacologically relevant trajectories. The line emerging from the origin is redrawn from figure 3, and is the locus of the combined effects of the volatile anesthetic on both the T-type Ca^{2+} channel and $GABA_A$ receptor as volatile anesthetic concentration is increased. For each given volatile anesthetic concentration, the coherence was determined. Isoboles were then generated by connecting this point with points on each axis where modulation of that channel, by itself, would lead to the same network behavior as measured by the coherence. For isoflurane (*A*), isoboles were generated for increments of 0.025 mM on the left and 0.0125 mM on the right. For halothane (*B*), isoboles were generated for increments of 0.04 mM on the left and 0.02 mM on the right. In all panels, *arrows* depict the volatile anesthetic concentrations corresponding to minimum alveolar concentration (MAC)-awake. Note the regions of synergy (concave with respect to origin), additivity (linear with respect to origin), and antagonism (convex with respect to origin). Isoboles corresponding to MAC-awake concentrations of isoflurane (*solid lines*) and halothane (*dashed lines*) are depicted in *C*. Here, χ^2 was 0.325 for isoflurane and 0.335 for halothane at MAC-awake. See text for details.

(SK), and assumptions about VA effects on the ion channels. The bias current was adjusted so that the network would oscillate at approximately 10 Hz with the neurons displaying appropriate individual bursting patterns.[33] For the network parameters used in the current study, network synchrony as determined by the coherence parameter introduced earlier varied biphasically with the bias current. As the amplitude of the bias current increased around the value of 0.12 nA, network synchrony increased with the magnitude of the bias current. When the bias current reached approximately 0.15 nA, network synchrony began to decline. Use of a random distribution of bias current amplitude altered network synchrony in no substantial way. As connectivity increased, so did network synchrony, and the value of 0.85 used for the fraction of total neurons to which each was connected represented a balance between starting with a poorly synchronized network and one that was so organized that VA-induced changes would be difficult to observe. Similarly, an increase in $GABA_A$ receptor conductance effectively enhanced connectivity and, therefore, network synchrony. The value used in the current simulations represents a balance between asynchronous network behavior and one whose activity in the control state is already highly organized. Inclusion of SK did not appreciatively alter network behavior when VA effects were introduced. Therefore, as in a number of other models of the RTN, it was not incorporated.[32,33] Furthermore, inclusion of the VA modulation of IPSP amplitude as depicted in figure 2C did not appreciatively alter network behavior over the range of VA concentrations studied and, therefore, was not further considered in the detailed studies.

Discussion

The simulations presented here demonstrate how relatively modest VA effects at T-type Ca^{2+} channels and $GABA_A$ receptors, individually and jointly, can alter the behavior of a computational model of the RTN. That effects at multiple sites can individually lead to similar alterations in network behavior may help to explain why point mutations of the $GABA_A$ receptor, while largely

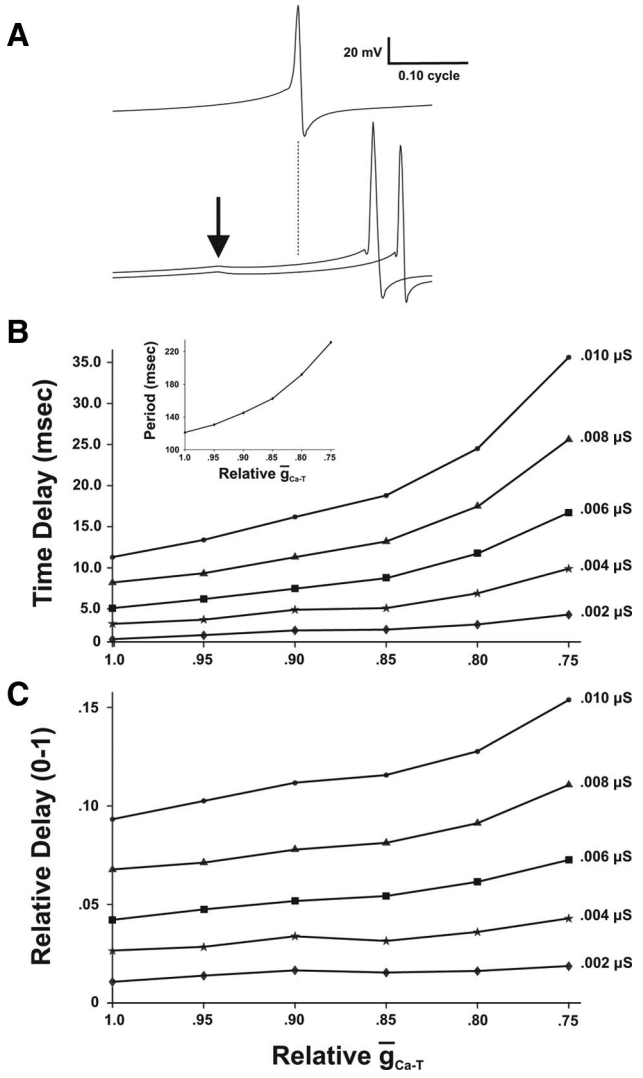

Fig. 8. Decreasing T-type Ca^{2+} conductance potentiates delay until next burst produced by a pulse of γ-aminobutyric acid (GABA) in individual model neurons isolated from the network. In the example in *A*, a burst consisting of a single spike is shown at the top for a single unperturbed neuron excited by steady current injection. Onset of the burst is delayed by a pulse of GABA (0.5 mM GABA, 0.3 ms duration, with $GABA_A$ conductance of 0.01 μS), applied at the *arrow* under control conditions (*left*) and further delayed when the T-type Ca^{2+} conductance is reduced to 0.8 of its control value. In *A*, the time axis was adjusted so that each neuron has a cycle length of 1.0 and the pulse was applied at 0.9, where 0 corresponds to the peak of the first spike. The delay as the T-type Ca^{2+} conductance is decreased is systematically explored in *B* and *C* for increasing levels of the $GABA_A$ conductance. Here, 0.002 μS corresponds to approximately the conductance of a single model synapse. Absolute delays in burst onset with a pulse of $GABA_A$ are shown in *B* along with inset depicting how cycle length increases with decrements in T-type Ca^{2+} conductance. Relative delays in cycle length are shown in *C*. Note how decrements in T-type Ca^{2+} conductance increase delays, as does an increase in $GABA_A$ conductance, as would occur from multiple presynaptic pulses occurring in unison.

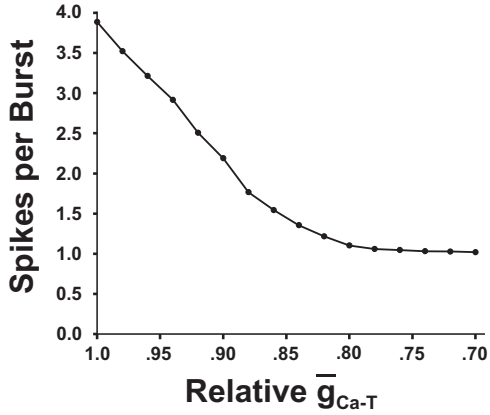

Fig. 9. Role of T-type Ca^{2+} conductance on burst length. As conductance decreases, the average number of spikes in a burst also decreases from those shown in the examples of figure 1B and less directly in figure 4A, effectively decreasing the strength of inhibitory network interactions because each spike produces a synaptic pulse of γ-aminobutyric acid (GABA) in the model. Note that as the number of spikes per burst plateaus, but decreases in Ca^{2+} conductance continue to influence entrainment properties of the network (fig. 8), there is a steep increase in the influence of Ca^{2+} conductance on network coherence (fig. 6A), and the isobolograms (fig. 7) depict some synergistic behavior. The SE of the means from three separate simulations is 0.03 spikes or less for each of the points shown.

abolishing some animal behaviors in the presence of IAs, minimally affected those observed in the presence of VAs.[45] These VA effects enhanced the synchrony of the neurons in the network and, when considered jointly, the combination was largely additive with some deviations toward mild synergism or antagonism depending on VA concentration and the choice of VA. As demonstrated in figure 8, VA-induced decrements in the T-type Ca^{2+} current potentiated the effects of GABA. This interaction was limited as VA concentration increased because this same VA effect on the T-type Ca^{2+} current led to reductions in burst length, as shown in figure 9, and reduced the amount of inhibition generated by that burst. Overall, the VAs isoflurane and halothane, despite substantially different potencies with respect to immobility and consciousness, produced similar levels of network synchrony at VA concentrations corresponding to clinical measures of MAC-awake in humans.

These computational studies were motivated by the role of the thalamus in consciousness and evidence that thalamic behavior is altered at VA concentrations capable of producing unconsciousness.[23,46–48] Implicit in the hypothesis that VAs produce unconsciousness by modulation of thalamic activity is the assumption that thalamic neurons are particularly vulnerable to the modulation of ion channel behavior produced by VAs. Thalamic neurons are somewhat unique in that their intrinsic behavior is dominated by low-voltage–activated Ca^{2+} channels.[32] $GABA_A$ inhibitory interactions contribute to network behavior, particularly in the RTN.[29] Therefore, it is consistent with the hypothesis of thalamic involvement in VA-induced unconsciousness that VAs modulate the activity of both T-type Ca^{2+} channels and $GABA_A$ receptors (fig. 2). This hypothesis is further supported by the observation, also illustrated in figure 2, that VA sensitivity of the key ion channels of the thalamus is,

overall, greater for isoflurane than for halothane. Although halothane is more potent with respect to immobility (MAC), isoflurane is more potent with respect to consciousness (MAC-awake), particularly when MAC-awake is expressed in terms of MAC (0.25 for isoflurane and 0.59 for halothane).[15] Therefore, as shown in figure 3, MAC-awake concentrations of the two VAs lie close to one another when considering the joint VA effect on T-type Ca^{2+} channels and $GABA_A$ receptors. Nonetheless, as also seen in figure 3, the relative modulation of the thalamic ion channels at MAC-awake concentrations differs somewhat between the two VAs, suggesting that their joint impact on thalamic behavior should be considered. When this was done by quantifying the synchrony of network activity within the model RTN, the impact on network behavior was similar for the two VAs. Collectively, these results are consistent with clinical and laboratory data that identify the thalamus as a site of VA-induced unconsciousness, and that VA modulation of both voltage- and ligand-gated ion channels contributes.

The isobolographic analysis of figure 7 demonstrated that the joint effect of the VAs on network synergy was largely additive, with some small deviations toward synergism or antagonism. As shown in figure 8, the ability of VA-induced decrements in the T-type Ca^{2+} current to enhance network synchrony seems to lie in their ability to augment the impact of inhibitory pulses mediated by $GABA_A$ receptors at times when the Ca^{2+} current was active. Qualitative differences in the isobolograms likely reflects the different balance in effects on T-type Ca^{2+} and $GABA_A$ currents illustrated for the two VAs in figures 2 and 3.

Values for MAC-awake differ somewhat as a function of the study and target population in those studies. For example, just as with MAC, MAC-awake decreases with age, though maintaining a similar proportion to MAC.[49] The values used in the current study for MAC-awake (0.25 MAC for isoflurane and 0.59 MAC for halothane)[15] have the merit of being determined in a single study. These values are similar to those from other studies (*e.g.*, 0.55 MAC for halothane[16] and 0.317–0.364 MAC for isoflurane[17–20]). The slightly smaller value for halothane and slightly larger ones for isoflurane than those used in the current study would lead to even greater similarity in the values of network coherence obtained for MAC-awake, as can be seen in figure 6F, where network coherence varies monotonically with VA concentration.

Suitability of Network Model

When compared with the entire brain or even the most detailed thalamocortical models,[50] the model used in the current study is relatively simple. Enhancements might include interactions with other brain regions, multicompartment models of individual neurons that replicate the detailed dendritic structure of the neurons and the spatial distribution of ion channels over those dendrites, and a full complement of known ion channels. Although all models represent a compromise between absolute reality, availability of data to configure the model, solubility of the model, and the outstanding question the model is intended to answer, each of these candidate modifications are of potential significance.

The RTN modulates and, in turn, is modulated by a number of other brain regions,[29] and is an important regulator of thalamic oscillations.[36] The RTN inhibits thalamic relay neurons and receives excitatory input from them. Thalamic relay neurons project the majority of the input from sensory organs to the cerebral cortex, leading to excitation of the cerebral cortex, which then provides excitatory feedback to both the RTN and thalamic relay neurons. Apart from its impact on network interactions, excitation of thalamic neurons due to feedback from the cortex could substantially alter the intrinsic behavior of individual neurons by increasing membrane potential so that the T-type Ca^{2+} channels can no longer de-inactivate. Therefore, it should not be surprising that models including all of these structures have demonstrated important interactions,[51] that functional imaging demonstrates that sedative levels of VAs alter interactions between these structures,[23,47] and that recordings from these structures during anesthesia demonstrate the importance of corticothalamic feedback loops.[52]

Even if feedback from other brain structures did not substantially alter thalamic behavior, a more comprehensive model would still be important. First, thalamic electrical activity, as opposed to cortical electroencephalographic activity, is not generally accessible during clinical practice. Therefore, clinical correlates of model predications could require cortical electroencephalograms generated by a model that incorporated corticothalamic interactions. Second, even though the current model demonstrated an enhancement of network synchrony with increasing anesthetic concentrations and identified the level of model synchrony associated with MAC-awake concentrations of the VAs, it was not immediately clear why this level of synchrony might be associated with unconsciousness. A fundamental qualitative change in model behavior as VA concentration is increased, the bifurcation seen in more abstract models of anesthetic action,[53] might only be observable in a model with a cortical component driven by an increasingly synchronized thalamus.

Although represented in the current model as a single compartment, neurons are complex structures with elaborate dendritic arbors, often requiring models with hundreds of compartments to capture this level of detail. Thalamic neurons are no exception, with models containing up to several hundred compartments.[31,32] Such models have demonstrated the importance of dendritic anatomy in replicating the details of bursting in thalamic

neurons. However, much of this detail can be captured in models with as few as three compartments using algorithms designed to generate reduced models from the anatomically more complex ones.[32] Some of the fidelity of the three-compartment models to physiologically determined burst trajectories is lost when such models are reduced to a single compartment.[32] Nonetheless, such models do replicate a considerable portion of the known physiology, particularly what is necessary to assess their contribution to network behavior. One of the major differences, though of limited impact with respect to the current study, which is driven by relative VA-induced decrements in conductances, is that larger values of the T-type Ca^{2+} conductance are necessary in the reduced models. One potential limitation of using anatomically detailed models of individual neurons, apart from the computational burden this imposes, is that this requires additional assumptions regarding connectivity of proximal and distal compartments of their respective dendritic trees. Such detailed models would also require assumptions regarding the distribution of conductances along the dendritic tree.

Apart from the anatomic detail of individual neurons and their connections, the role of ion channels not included in the simulations needs to be considered. With respect to voltage-gated channels, the current model is somewhat parsimonious, using a T-type Ca^{2+} channel, with fast Na^+ and K^+ channels to generate spikes. This combination of channels has been shown to be sufficient to generate realistic bursting behavior in models of individual neurons, particularly in multicompartment models.[32,33] The small Ca^{2+}-activated K^+ channel (SK) is known to contribute to the behavior of reticular neurons by producing an afterhyperpolarization that facilitates de-inactivation of the T-type Ca^{2+} channels.[29] It is conceivable that VA modulation of Ca^{2+} entry *via* the T-type Ca^{2+} channels could decrease internal Ca^{2+} concentration, leading to a decrease in the current produced by SK. However, inclusion of SK did not substantially alter network behavior for the VA concentrations studied here and, therefore, it was not included. Another conductance that is present in reticular neurons[54] and depends on intracellular Ca^{2+} concentration, but has slower kinetics than SK, is the calcium-activated nonspecific cation current.[55] Through this channel, an increase in intracellular Ca^{2+} concentration leads to depolarization and a shift from bursting to tonic spiking as the T-type Ca^{2+} channel becomes inactivated. Again, this channel was not incorporated because large network simulations have not found it to be necessary,[33] and because SK with an opposite but faster effect was also not incorporated. Importantly, neither of these conductances are known to be directly modulated by VAs.

Another class of ion channel not incorporated is the hyperpolarization-activated cyclic nucleotide-gated (HCN) channels, which have recently been shown to be present in reticular neurons.[56] Because these channels seem to play a role in integrating signals from spatially disparate locations along the dendritic tree,[57] their inclusion would likely be necessary when considering multicompartment models with realistic dendritic anatomy. Halothane is known to affect HCN channels,[58] including HCN2, an isoform known to be present on reticular neurons.[56,59] However, for the concentrations used in the current study, the effects of halothane on HCN2 are small,[58] but of undetermined impact on model behavior. Members of the two-pore domain K^+ channel family can also be localized to the reticular nucleus[60] and, of those, several are modulated by VAs.[61,62] In contrast to VA effects on the T-type Ca^{2+} channel, VAs increase K^+ conductance of the two-pore domain K^+ channels. However, the impact on network activity of VAs increasing the hyperpolarizing current produced by these channels may be complex, as indicated by recent experiments demonstrating how these channels can actually increase neural firing.[63]

Although $GABA_A$ receptors were incorporated in the model, extrasynaptic $GABA_A$ receptors are also known to reside in the thalamus.[64,65] In contrast to $GABA_A$ receptors at the synapse, extrasynaptic $GABA_A$ receptors generate tonic inhibitory currents.[64–66] These inhibitory currents are enhanced by the IAs[67,68] and the VA isoflurane.[69] Therefore, inclusion of extrasynaptic $GABA_A$ receptors in the model would introduce an inhibitory current that would increase with introduction of many types of IAs and VAs. This inhibitory current would effectively reduce the level of excitatory bias current in the model or, at higher levels, even produce a net inhibitory effect. As indicated in Results, this would actually reduce network synchrony because it would tend to reduce spiking during a burst, leading to less inhibition of other members of the network. However, because the response to the excitatory bias current is biphasic, for higher levels of excitatory input network the addition of an inhibitory current will cause network synchrony to increase. At higher levels of excitatory input, inhibition reduces burst frequency, making it easier to synchronize the network,[70] particularly when the anesthetics are simultaneously increasing the deactivation time of the synaptic $GABA_A$ receptors. These issues may also be important when considering the excitatory feedback to the RTN from thalamocortical relay neurons and the cortex.

VA Modulation of Ion Channel Behavior

The current studies are heavily dependent on data regarding VA modulation of multiple ion channels by multiple VAs. Of the data used in the current study, the greatest degree of uncertainty lay in the effect of halothane on $GABA_A$ receptor activity because, as described in the figure and accompanying text, the function in figure 2 was obtained from limited data pooled from multiple sources.[8,34,35] It is conceivable that better data

could lead to even greater similarity in behavior of isoflurane and halothane at MAC-awake concentrations. One aspect of VA effects on $GABA_A$ receptors that was not incorporated into the principal simulations was the decrease in the amplitude of the IPSP produced by GABA and depicted in figure 2C. This effect differed little from unity over the range of anesthetics studied in the simulations presented here. When both VA-induced increases in the time constant governing deactivation of the $GABA_A$ channel and the decrease in IPSP amplitude were simultaneously incorporated, for the range of VA concentrations under consideration, the impact on model coherence was not discernable from results obtained when only the effect related to the rate of $GABA_A$ deactivation was included. Some of this relates to the fact that although equivalent from the standpoint of net inhibitory charge transfer, the product of the decrement in IPSP amplitude and increases in the time constant governing channel deactivation, these two effects are not equivalent in their impact on network behavior. Increases in the time constant governing $GABA_A$ receptor deactivation is more effective at increasing network synchrony than an increase in IPSP amplitude that is equivalent with respect to inhibitory charge transfer (A. Gottschalk, M.D., Ph.D., and S. A. Miotke, M.S., Baltimore, Maryland, unpublished computer simulations, 2007), which is consistent with more general studies of how synaptic decay time affects network synchronization.[70] However, net charge transfer may be more relevant for tonic, as opposed to phasic, inhibitory input as might occur from extrasynaptic $GABA_A$ receptors in the thalamus.[69]

Whether the results governing network behavior, like those in the upper right panels of figure 5 and that of figure 6B, are sufficient to account for the behavior of the IAs that act principally at the $GABA_A$ receptor remains to be established. Computational approaches have already demonstrated the importance of inhibitory interactions in network synchronization[71–73] and established that increases in the time constant for $GABA_A$ receptor deactivation can alter network behavior in computational models of the hippocampus,[74] sensory cortex,[72] and RTN.[42] However, prolongation in the time constant for $GABA_A$ receptor deactivation can also reduce synchronization,[21,73] particularly in networks with higher intrinsic frequency.[70] The data of figure 6B indicate that a prolongation in the time constant for $GABA_A$ receptor deactivation of approximately 50% achieves the same level of network synchrony as seen for MAC-awake concentrations of the VAs considered in this study. Although the available direct experimental data on $GABA_A$ kinetics at IA concentrations associated with loss of consciousness are sparse, this observation from the model is consistent with the relative changes in $GABA_A$ kinetics imputed from recordings in hippocampal slice preparations.[74] In these studies, ED_{50} concentrations of propofol (2.8 μg/ml)[75] and sodium thiopental (15.6 μg/ml)[76] for loss of consciousness are associated with an approximately 50% increase in the time constant for $GABA_A$ receptor deactivation. However, the IAs do more than prolong $GABA_A$ deactivation. Like the VAs, the IAs can decrease the amplitude of $GABA_A$ receptor IPSPs.[77,78] The quantitative extent that decreases in IPSP amplitude associated with the IAs affect network behavior was not determined, but these effects would be expected to decrease network synchrony to some extent. Importantly, other IA effects could conceivably play a critical role, as suggested by animal studies where point mutations of the $GABA_A$ receptor abolish the response to noxious stimuli and reduce but do not abolish the loss of righting reflex.[45] For example, propofol may inhibit SK activity in neurons of the RTN,[79] leading to enhanced excitability of these neurons. Propofol can also block HCN channels in neurons of the RTN, enhancing the impact of postsynaptic potentials at the soma, but also interfering with the integrative properties of the dendritic network.[59] Therefore, to more fully account for IA effects, model enhancements may require not only the inclusion of additional channels such as SK and one or more HCN subtypes, but also a more realistic dendritic arbor to address the impact of HCN modulation on the integrative properties of the dendrites.

Characterizing Network Behavior

To construct the isobolograms and to evaluate the effect of parameter variations in general, it was necessary to be able to characterize network behavior with a single continuous parameter with some degree of physiologic relevance. The choice of network synchrony and the specific synchrony measure require explanation. It is synchronization of the electrical activity of multiple neurons that leads to the organized pattern of electrical activity seen with electroencephalography and with depth electrodes. Such organization contributes to the slowing and increased amplitude of the waveform that characterizes the electroencephalogram as anesthetic depth is increased.[22] However, loss of synchronized activity among neurons of higher-frequency ranges (*e.g.*, gamma) could also contribute to slowing of the electroencephalogram and is known to occur in hippocampal slice with IAs.[80] The process whereby anesthetic-induced alterations in the organization of thalamic activity could alter the cortical electroencephalogram is complex and seems to depend on corticothalamic feedback loops.[48,51] Therefore, an appreciation for this process will minimally require more elaborate models that incorporate these elements. Nonetheless, although many variations are known, synchronization of neural activity with administration of general anesthetics is an empiric observation.

There are many theoretical and practical issues involved in the choice of a synchrony measure which

preclude the existence of an ideal measure.[81] One, used in many theoretical studies of coupled sinusoidal oscillators, examines the phase of each oscillator by representing it as a point on the unit circle in the complex plane.[82] Network synchrony is determined by essentially taking the average distance from the center of the unit circle. This straightforward approach underlies the histograms of relative phase given in figure 5. However, there are several potential pitfalls. The first is that highly organized subgroups that are 180° out of phase will seem no more organized than a system with random phase. Such issues can be readily addressed, but examination of the histograms of relative phase in the current study indicated that this was not an overwhelming issue. The second is that by considering phase only, a large number of low-amplitude signals could dominate the synchrony measure. The synchrony measure used in the current study[42] effectively considers both phase and amplitude information about the individual neural trajectories. Moreover, it does so over the entire frequency range of the neuron's trajectory, rather than just at a dominant or otherwise chosen frequency. Eventually, rather than using such abstract measures, models should be directly comparable with experimentally determined electroencephalograms.

Conclusions

Despite limitations on the data characterizing the interaction of multiple VAs at multiple receptors, the imprecision of clinical endpoints such as MAC-awake, the use of a somewhat parsimonious model of a single thalamic nucleus, and the use of an abstract measure to characterize model behavior, a somewhat coherent picture emerges from the foregoing studies. These studies demonstrated how relatively small, but established, VA effects at multiple sites in a neurobiologically relevant location of the central nervous system could combine in a predominately additive fashion to alter model behavior at VA concentrations corresponding to MAC-awake. The appropriateness of the choice of model, the adequacy of the data used to drive the model, and the utility of the measure of model behavior are supported by the ability to obtain a similar effect with the model when using MAC-awake concentrations of VAs with markedly different clinical potencies. It is expected that the picture painted by modeling studies will become clearer and more relevant as additional laboratory data about VA interaction with ion channels become available, models are expanded to consider additional anesthetic effects due to both VAs and IAs, and such models generate outputs that can readily be contrasted with data obtained *in vivo*.

The authors thank Peter A. Goldstein, M.D. (Associate Professor, Department of Anesthesiology, Weill Cornell Medical College, New York, New York), and Marek A. Mirski, M.D., Ph.D. (Associate Professor, Department of Anesthesiology and Critical Care Medicine, Johns Hopkins Hospital, Baltimore, Maryland), for their many valuable suggestions.

References

1. Campagna JA, Miller KW, Forman SA: Mechanisms of actions of inhaled anesthetics. N Engl J Med 2003; 348:2110–24
2. Franks NP: General anaesthesia: From molecular targets to neuronal pathways of sleep and arousal. Nat Rev Neurosci 2008; 9:370–86
3. Eger EI, Saidman LJ, Brandstater B: Minimum alveolar anesthetic concentration: A standard of anesthetic potency. ANESTHESIOLOGY 1965; 26:756–63
4. Franks NP, Lieb WR: Molecular and cellular mechanisms of general anaesthesia. Nature 1994; 367:607–14
5. Herrington J, Stern RC, Evers AS, Lingle CJ: Halothane inhibits two components of calcium current in clonal (GH3) pituitary cells. J Neurosci 1991; 11: 2226–40
6. Todorovic SM, Lingle CJ: Pharmacological properties of T-type Ca2+ current in adult rat sensory neurons: Effects of anticonvulsant and anesthetic agents. J Neurophysiol 1998; 79:240–52
7. Kameyama K, Aono K, Kitamura K: Isoflurane inhibits neuronal Ca2+ channels through enhancement of current inactivation. Br J Anaesth 1999; 82:402–11
8. Banks MI, Pearce RA: Dual actions of volatile anesthetics on GABA(A) IPSCs: Dissociation of blocking and prolonging effects. ANESTHESIOLOGY 1999; 90:120–34
9. Jones MV, Brooks PA, Harrison NL: Enhancement of gamma-aminobutyric acid-activated Cl- currents in cultured rat hippocampal neurones by three volatile anaesthetics. J Physiol 1992; 449:279–93
10. Harrison NL, Kugler JL, Jones MV, Greenblatt EP, Pritchett DB: Positive modulation of human gamma-aminobutyric acid type A and glycine receptors by the inhalation anesthetic isoflurane. Mol Pharmacol 1993; 44:628–32
11. MacIver MB, Tanelian DL, Mody I: Two mechanisms for anesthetic-induced enhancement of GABAA-mediated neuronal inhibition. Ann N Y Acad Sci 1991; 625:91–6
12. Hales TG, Lambert JJ: The actions of propofol on inhibitory amino acid receptors of bovine adrenomedullary chromaffin cells and rodent central neurones. Br J Pharmacol 1991; 104:619–28
13. Proctor WR, Mynlieff M, Dunwiddie TV: Facilitatory action of etomidate and pentobarbital on recurrent inhibition in rat hippocampal pyramidal neurons. J Neurosci 1986; 6:3161–8
14. Barker JL, Harrison NL, Lange GD, Owen DG: Potentiation of gamma-aminobutyric-acid-activated chloride conductance by a steroid anaesthetic in cultured rat spinal neurones. J Physiol 1987; 386:485–501
15. Gaumann DM, Mustaki JP, Tassonyi E: MAC-awake of isoflurane, enflurane and halothane evaluated by slow and fast alveolar washout. Br J Anaesth 1992; 68:81–4
16. Stoelting RK, Longnecker DE, Eger EI: Minimum alveolar concentrations in man on awakening from methoxyflurane, halothane, ether and fluroxene anesthesia: MAC awake. ANESTHESIOLOGY 1970; 33:5–9
17. Dwyer R, Bennett HL, Eger EI, Heilbron D: Effects of isoflurane and nitrous oxide in subanesthetic concentrations on memory and responsiveness in volunteers. ANESTHESIOLOGY 1992; 77:888–98
18. Katoh T, Suguro Y, Kimura T, Ikeda K: Cerebral awakening concentration of sevoflurane and isoflurane predicted during slow and fast alveolar washout. Anesth Analg 1993; 77:1012–7
19. Katoh T, Suguro Y, Ikeda T, Kazama T, Ikeda K: Influence of age on awakening concentrations of sevoflurane and isoflurane. Anesth Analg 1993; 76:348–52
20. Goto T, Nakata Y, Ishiguro Y, Niimi Y, Suwa K, Morita S: Minimum alveolar concentration-awake of xenon alone and in combination with isoflurane or sevoflurane. ANESTHESIOLOGY 2000; 93:1188–93
21. Gottschalk A, Haney P: Computational aspects of anesthetic action in simple neural models. ANESTHESIOLOGY 2003; 98:548–64
22. Levy WJ: Neurophysiologic brain monitoring: Electroencephalography, Anesthesia and Neurosurgery, 4th edition. Edited by Cottrell JE, Smith DS. Philadelphia, Mosby, 2001, pp 201–17
23. Alkire MT, Haier RJ, Fallon JH: Toward a unified theory of narcosis: Brain imaging evidence for a thalamocortical switch as the neurophysiologic basis of anesthetic-induced unconsciousness. Conscious Cogn 2000; 9:370–86
24. Antognini JF, Schwartz K: Exaggerated anesthetic requirements in the preferentially anesthetized brain. ANESTHESIOLOGY 1993; 79:1244–9
25. Zhang Y, Laster MJ, Hara K, Harris RA, Eger EI, Stabernack CR, Sonner JM: Glycine receptors mediate part of the immobility produced by inhaled anesthetics. Anesth Analg 2003; 96:97–101
26. Steriade M, Deschenes M: The thalamus as a neuronal oscillator. Brain Res 1984; 320:1–63
27. Deschenes M, Paradis M, Roy JP, Steriade M: Electrophysiology of neurons of lateral thalamic nuclei in cat: Resting properties and burst discharges. J Neurophysiol 1984; 51:1196–219
28. Alkire MT, Pomfrett CJ, Haier RJ, Gianzero MV, Chan CM, Jacobsen BP, Fallon JH: Functional brain imaging during anesthesia in humans: Effects of

halothane on global and regional cerebral glucose metabolism. ANESTHESIOLOGY 1999; 90:701–9
29. Sherman SM, Guillery RW: Exploring the Thalamus. San Diego, Academic Press, 2001, pp 109–68
30. Sejnowski TJ, Destexhe A: Why do we sleep? Brain Res 2000; 886:208–23
31. Destexhe A, Neubig M, Ulrich D, Huguenard J: Dendritic low-threshold calcium currents in thalamic relay cells. J Neurosci 1998; 18:3574–88
32. Destexhe A, Contreras D, Steriade M, Sejnowski TJ, Huguenard JR: *In vivo*, *in vitro*, and computational analysis of dendritic calcium currents in thalamic reticular neurons. J Neurosci 1996; 16:169–85
33. Destexhe A, Bal T, McCormick DA, Sejnowski TJ: Ionic mechanisms underlying synchronized oscillations and propagating waves in a model of ferret thalamic slices. J Neurophysiol 1996; 76:2049–70
34. Jones MV, Harrison NL: Effects of volatile anesthetics on the kinetics of inhibitory postsynaptic currents in cultured rat hippocampal neurons. J Neurophysiol 1993; 70:1339–49
35. Kitamura A, Marszalec W, Yeh JZ, Narahashi T: Effects of halothane and propofol on excitatory and inhibitory synaptic transmission in rat cortical neurons. J Pharmacol Exp Ther 2003; 304:162–71
36. Sohal VS, Huntsman MM, Huguenard JR: Reciprocal inhibitory connections regulate the spatiotemporal properties of intrathalamic oscillations. J Neurosci 2000; 20:1735–45
37. Destexhe A, Contreras D, Sejnowski TJ, Steriade M: A model of spindle rhythmicity in the isolated thalamic reticular nucleus. J Neurophysiol 1994; 72:803–18
38. Nikonorov IM, Blanck TJ, Recio-Pinto E: The effects of halothane on single human neuronal L-type calcium channels. Anesth Analg 1998; 86:885–95
39. Wolfram S: The Mathematica Book, 4th edition. New York, Cambridge University Press, 1999
40. Bower JM, Beeman D: The Book of GENESIS: Exploring Realistic Neural Models with the General Neural Simulation System, 2nd edition. New York, Springer-Verlag, 1998
41. Marple SL: Digital Spectral Analysis with Applications. Englewood Cliffs, New Jersey, Prentice-Hall, 1987, pp 130–71
42. Golomb D, Rinzel J: Clustering in globally coupled inhibitory neurons. Physica D 1994; 72:259–82
43. Gessner PK: Isobolographic analysis of interactions: An update on applications and utility. Toxicology 1995; 105:161–79
44. McAdam LC, MacDonald JF, Orser BA: Isobolographic analysis of the interactions between midazolam and propofol at $GABA_A$ receptors in embryonic mouse neurons. ANESTHESIOLOGY 1998; 89:1444–54
45. Jurd R, Arras M, Lambert S, Drexler B, Siegwart R, Crestani F, Zaugg M, Vogt KE, Ledermann B, Antkowiak B, Rudolph U: General anesthetic actions *in vivo* strongly attenuated by a point mutation in the GABA(A) receptor beta3 subunit. FASEB J 2003; 17:250–2
46. Llinas R, Ribary U: Consciousness and the brain: The thalamocortical dialogue in health and disease. Ann N Y Acad Sci 2001; 929:166–75
47. White NS, Alkire MT: Impaired thalamocortical connectivity in humans during general-anesthetic-induced unconsciousness. Neuroimage 2003; 19:402–11
48. Hayashi K, Sawa T, Matsuura M: Anesthesia depth–dependent features of electroencephalographic bicoherence spectrum during sevoflurane anesthesia. ANESTHESIOLOGY 2008; 108:841–50
49. Eger EI: Age, minimum alveolar anesthetic concentration, and minimum alveolar anesthetic concentration-awake. Anesth Analg 2001; 93:947–53
50. Izhikevich EM, Edelman GM: Large-scale model of mammalian thalamocortical systems. Proc Natl Acad Sci U S A 2008; 105:3593–8
51. Destexhe A, Contreras D, Steriade M: Mechanisms underlying the synchronizing action of corticothalamic feedback through inhibition of thalamic relay cells. J Neurophysiol 1998; 79:999–1016
52. Velly LJ, Rey MF, Bruder NJ, Gouvitsos FA, Witjas T, Regis JM, Peragut JC, Gouin FM: Differential dynamic of action on cortical and subcortical structures of anesthetic agents during induction of anesthesia. ANESTHESIOLOGY 2007; 107:202–12
53. Steyn-Ross ML, Steyn-Ross DA, Sleigh JW, Liley DTJ: Theoretical electroencephalogram stationary spectrum for a white-noise-driven cortex: Evidence for a general anesthetic-induced phase transition. Phys Rev E 1999; 60:7299–311
54. Bal T, McCormick DA: Mechanisms of oscillatory activity in guinea-pig nucleus reticularis thalami *in vitro*: A mammalian pacemaker. J Physiol 1993; 468:669–91
55. Partridge LD, Swandulla D: Calcium-activated non-specific cation channels. Trends Neurosci 1988; 11:69–72
56. Abbas SY, Ying SW, Goldstein PA: Compartmental distribution of hyperpolarization-activated cyclic-nucleotide-gated channel 2 and hyperpolarization-activated cyclic-nucleotide-gated channel 4 in thalamic reticular and thalamocortical relay neurons. Neuroscience 2006; 141:1811–25
57. Robinson RB, Siegelbaum SA: Hyperpolarization-activated cation currents: From molecules to physiological function. Annu Rev Physiol 2003; 65:453–80
58. Chen X, Sirois JE, Lei Q, Talley EM, Lynch C III, Bayliss DA: HCN subunit-specific and cAMP-modulated effects of anesthetics on neuronal pacemaker currents. J Neurosci 2005; 25:5803–14
59. Ying SW, Jia F, Abbas SY, Hofmann F, Ludwig A, Goldstein PA: Dendritic HCN2 channels constrain glutamate-driven excitability in reticular thalamic neurons. J Neurosci 2007; 27:8719–32
60. Talley EM, Solorzano G, Lei Q, Kim D, Bayliss DA: CNS distribution of members of the two-pore-domain (KCNK) potassium channel family. J Neurosci 2001; 21:7491–505
61. Patel AJ, Honore E, Lesage F, Fink M, Romey G, Lazdunski M: Inhalational anesthetics activate two-pore-domain background K+ channels. Nat Neurosci 1999; 2:422–6
62. Andres-Enguix I, Caley A, Yustos R, Schumacher MA, Spanu PD, Dickinson R, Maze M, Franks NP: Determinants of the anesthetic sensitivity of two-pore domain acid-sensitive potassium channels: Molecular cloning of an anesthetic-activated potassium channel from Lymnaea stagnalis. J Biol Chem 2007; 282:20977–90
63. Brickley SG, Aller MI, Sandu C, Veale EL, Alder FG, Sambi H, Mathie A, Wisden W: TASK-3 two-pore domain potassium channels enable sustained high-frequency firing in cerebellar granule neurons. J Neurosci 2007; 27:9329–40
64. Cope DW, Hughes SW, Crunelli V: GABAA receptor-mediated tonic inhibition in thalamic neurons. J Neurosci 2005; 25:11553–63
65. Jia F, Pignataro L, Schofield CM, Yue M, Harrison NL, Goldstein PA: An extrasynaptic GABAA receptor mediates tonic inhibition in thalamic VB neurons. J Neurophysiol 2005; 94:4491–501
66. Wafford KA, van Niel MB, Ma QP, Horridge E, Herd MB, Peden DR, Belelli D, Lambert JJ: Novel compounds selectively enhance delta subunit containing GABA(A) receptors and increase tonic currents in thalamus. Neuropharmacology 2009; 56:182–9
67. Meera P, Olsen RW, Otis TS, Wallner M: Etomidate, propofol and the neurosteroid THDOC increase the GABA efficacy of recombinant alpha4beta3delta and alpha4beta3 GABA(A) receptors expressed in HEK cells. Neuropharmacology 2009; 56:155–60
68. Belelli D, Peden DR, Rosahl TW, Wafford KA, Lambert JJ: Extrasynaptic GABAA receptors of thalamocortical neurons: A molecular target for hypnotics. J Neurosci 2005; 25:11513–20
69. Jia F, Yue M, Chandra D, Homanics GE, Goldstein PA, Harrison NL: Isoflurane is a potent modulator of extrasynaptic GABA(A) receptors in the thalamus. J Pharmacol Exp Ther 2008; 324:1127–35
70. White JA, Chow CC, Ritt J, Soto-Trevino C, Kopell N: Synchronization and oscillatory dynamics in heterogeneous, mutually inhibited neurons. J Comput Neurosci 1998; 5:5–16
71. Lewis TJ, Rinzel J: Dynamics of spiking neurons connected by both inhibitory and electrical coupling. J Comput Neurosci 2003; 14:283–309
72. Merriam EB, Netoff TI, Banks MI: Bistable network behavior of layer I interneurons in auditory cortex. J Neurosci 2005; 25:6175–86
73. Wang XJ, Buzsaki G: Gamma oscillation by synaptic inhibition in a hippocampal interneuronal network model. J Neurosci 1996; 16:6402–13
74. Whittington MA, Jefferys JG, Traub RD: Effects of intravenous anaesthetic agents on fast inhibitory oscillations in the rat hippocampus *in vitro*. Br J Pharmacol 1996; 118:1977–86
75. Irwin MG, Hui TW, Milne SE, Kenny GN: Propofol effective concentration 50 and its relationship to bispectral index. Anaesthesia 2002; 57:242–8
76. Hung OR, Varvel JR, Shafer SL, Stanski DR: Thiopental pharmacodynamics, II: Quantitation of clinical and electroencephalographic depth of anesthesia. ANESTHESIOLOGY 1992; 77:237–44
77. Birnir B, Tierney ML, Dalziel JE, Cox GB, Gage PW: A structural determinant of desensitization and allosteric regulation by pentobarbitone of the GABAA receptor. J Membr Biol 1997; 155:157–66
78. Gage PW, Robertson B: Prolongation of inhibitory postsynaptic currents by pentobarbitone, halothane and ketamine in CA1 pyramidal cells in rat hippocampus. Br J Pharmacol 1985; 85:675–81
79. Ying SW, Goldstein PA: Propofol-block of SK channels in reticular thalamic neurons enhances GABAergic inhibition in relay neurons 2. J Neurophysiol 2005; 93:1935–48
80. Faulkner HJ, Traub RD, Whittington MA: Disruption of synchronous gamma oscillations in the rat hippocampal slice: A common mechanism of anaesthetic drug action. Br J Pharmacol 1998; 125:483–92
81. Pinsky PF, Rinzel J: Synchrony measures for biological neural networks. Biol Cybern 1995; 73:129–37
82. Strogatz SH: From Kuramoto to Crawford: Exploring the onset of synchronization in populations of coupled oscillators. Physica D 2000; 143:1–20